ARTICLE

Detection of a miRNA biomarker for cancer diagnosis using SERS tags and magnetic separation

Received 00th January 20xx,
Accepted 00th January 20xx

DOI: 10.1039/x0xx00000x

Kiatnida Treerattrakoon,[a,c] Pimporn Roeksrungruang,[a] Tararaj Dharakul,[b] Deanpen Japrung,[a] Karen Faulds,[c] Duncan Graham,[c] and Suwussa Bamrungsap*[a]

Detection of miR-29a, a biomarker of cancers, using SERS tags and magnetic separation is described. The assay was designed to detect the miR-29a sequence by taking the complementary sequence and splitting it into a capture and detection probe. The SERS tags comprised the highly Raman active molecule 4- mercaptobenzoic acid (4-MBA) and DNA detection probes assembled onto the surface of gold nanorods (AuNRs) through the self-assembly process. The capture DNA conjugated magnetic nanoparticles (MNPs) were applied as capture probes. The detection was based on the hybridisation and sandwich complex formation. The resultant hybridisation-dependent complexes were recovered and enriched from the samples by magnetic separation. The enriched solution containing target miRNA hybridised with capture probes were dropped on a foil-covered slide to form a droplet for SERS analysis. A characteristic spectrum of 4-MBA was observed to indicate the presence of the miR-29a in the samples. The sensitivity of the assay is examined by measuring the SERS signal of the samples containing different concentrations of the miR-29a. The SERS intensity appears to increase with the concentration of miR-29a. The limit of detection (LOD) was found to be 10 pM without any amplification process. In addition, the selectivity and feasibility of the assay in complex media are evaluated with the non-target miRNAs comprising different sequences from the target miR-29a. The system was capable of detecting the target miR-29a specifically with high selectivity. These results suggest that this solution-based SERS platform has a significant capability for simple, sensitive, and selective miR-29a analysis.

Introduction

MicroRNAs (miRNAs) are small noncoding RNAs, usually 19-25 bases in size, which post-transcriptionally regulate gene expression by binding to a 3'-UTR (untranslated region) of the target mRNA.[1, 2] Several hundred miRNAs have been identified in humans to date. It is also known that the expression patterns of miRNAs are different under normal and disease conditions. Many miRNAs play an important role in disease development, such as diabetes,[3–5] heart diseases,[6,7] cervical cancer,[8–10] and lung cancer.[11–13] Therefore, miRNAs have emerged as a new class of biomarkers for disease diagnosis, monitoring of progression, and even as a therapeutic target.[14] However, the short size of miRNAs makes them highly challenging to detect and analyse compared to long DNA targets. Many well-established molecular biology laboratories can analyse miRNAs using conventional methods, which include northern blot,[15] reverse transcription-polymerase chain reaction (RT-PCR),[16] in situ hybridisation (ISH),[17] and microarray approaches.[18] Some conventional methods, such as northern blot, do not require expensive equipment, but the sensitivity is low.[14,19,20] The gold standard RT-PCR method has remarkably high sensitivity but requires sophisticated primer design and expensive equipment.

Over the past few years, several novel methods have been developed to improve sensitivity, specificity, and efficacy for miRNA analysis. These methods often involve the use of nanomaterials, signal amplification strategies such as isothermal exponential amplification,[21] rolling circle amplification (RCA),[22–24] or hybridisation chain reaction (HCR).[25] Although the amplification approach can provide high sensitivity for miRNA analysis, they still have some drawbacks such as laborious probe design and fabrication, time-consuming additional and wash steps and require expensive reagents and instruments.

Surface-enhanced Raman scattering (SERS) has recently become one of the promising techniques for miRNAs analysis due to its extra high sensitivity. Benchtop confocal Raman spectrometers are typically used for SERS analysis of biological samples in a liquid environment due to their high spatial and spectral resolution. The liquid sample containing miRNAs can be measured with a confocal Raman spectrometer in a 384-well plate, requiring a sample volume of 30.0 µL.[26] Recent studies have also demonstrated that samples concentrated into microdroplets (~2.5-5.0 µL) can be measured with a confocal Raman spectrometer.[27–29] The enriched microdroplet contains 3D SERS active hotspots that can be excited more than a 2D

[a] National Nanotechnology Center (NANOTEC), National Science and Technology Development Agency (NSTDA), Pathumthani 12120, Thailand.
[b] Department of Immunology, Faculty of Medicine Siriraj Hospital, Mahidol University, Bangkok 10700, Thailand.
[c] Department of Pure and Applied Chemistry, Technology and Innovation Centre, University of Strathclyde, 99 George Street, Glasgow, UK.
† See DOI: 10.1039/x0xx00000x

planar SERS substrate.[27] Thus, the microdroplet is also suitable for the detection of low-abundant biological samples such as miRNA and offers the advantage of more efficient interrogation of the bulk of the sample. Nevertheless, the cost and rigidity of the confocal Raman spectrometer are significant drawbacks for the widespread use of SERS analysis at a point-of-care analysis or a low resource facility. Several studies have explored the use of a portable or handheld Raman spectrometer containing a miniaturised laser source. Still, there are remaining limitations, such as the requirement of large sample volume[26] or solid substrates.[30] A fibre optic-based Raman spectrometer is a compromise between a confocal Raman spectrometer and a handheld Raman spectrometer in terms of spatial resolution and instrument cost. Fibre optic-based Raman spectroscopy is a well-recognised technique used extensively in pharmaceutical industries as it allows for remote analysis of samples in liquid, solid, or powder forms.[31] Various research groups also use the fibre optic Raman probe for in vivo and ex vivo clinical spectroscopy applications.[32] However, to the best of our knowledge, the fibre optic Raman probe has never been used to analyse miRNA in microdroplets before.

SERS utilises the ability of metallic nanostructures, typically silver or gold nanoparticles, to generate a strong electromagnetic field localised on the surface of the particles resulting in enhancement of signal intensity by many orders of magnitude. Driskell et al. reported a direct method for identifying miRNAs using silver nanorod array substrates.[33] Partial least squares (PLS) regression analysis was then used to quantitatively analyse miRNA profiles in multicomponent mixtures. An alternative approach for SERS-based miRNA detection can be achieved by using SERS tags, which are nanoparticles functionalised with Raman reporters and single-stranded DNA (ssDNA) probes. Specific binding between DNA probes and target miRNAs brings two or more SERS tags into close proximity, resulting in plasmonic coupling and providing an intense SERS signal at the gaps between SERS tags. This labelled detection approach allows the identification of miRNAs with high sensitivity and selectivity. Graham et al. and Qian et al. have demonstrated that the SERS signal of spherical nanoparticles functionalised with Raman reporters and DNA probes can be significantly enhanced when the nanoparticles assemble upon binding with target DNA.[34,35] Guven et al. have developed a SERS-based sandwich assay for miR-21 detection using a combination of a gold-coated slide and rod-shaped nanoparticles functionalised with Raman reporters and DNA probes as SERS tags.[36] These approaches all produce suspension-based measurement system without any separation steps, resulting in longer times for the result and a compromise in sensitivity due to the bulk of the sample not being interrogated.

To address these issues, magnetic nanoparticles (MNPs) conjugated with DNA probes can be applied to separate target miRNAs from the sample and enable SERS tags to assemble around the MNPs in the presence of targets through a sandwich complex formation. Therefore, many areas of high SERS intensity can be generated at the interstitial spaces between SERS tags assembly due to hybridisation-dependent recognition between the DNA probes and the target miRNAs, resulting in an intense SERS signal and high detection sensitivity. Zhang et al. demonstrated a SERS-based assay for the detection of miR-141 involving MNPs. miR-141 targets were captured by DNA probes conjugated on gold-coated MNPs and reporter probes attached on Raman-tagged gold nanoparticles. The hybridisation complexes were detected by SERS with a LOD of 100 fM.[37] The detection of miRNAs using a combination of gold-coated MNPs and silica-coated gold nanoparticles to prevent dissociation of the Raman molecules from the surface was also reported using a similar approach. High sensitivity with a femtomolar range of detection and multiplex analysis feasibility were demonstrated.[38]

This work demonstrates the development of a simple and sensitive SERS-based platform using magnetic capture to detect miR-29a. Several studies have demonstrated the clinical potential of miR-29a as a biomarker for cancer diagnostics. For examples, previous studies clearly indicated the upregulated expression of miR-29a in serum of patients with colorectal cancer[39] and breast cancer[40] about 1.5-2 times compared to healthy people. The downregulation of miR-29a was found in hepatocellular carcinoma, acute myeloid leukemia, and non-small cell lung cancer.[41–42] The miR-29a is first captured by MNPs conjugated with ssDNA probes that recognise a section of the target sequence and then labelled by SERS tags which can partially hybridise to the other half of the target. The resultant hybridisation complexes are concentrated and dropped onto a microscope glass side covered with aluminium foil to form a microdroplet. The SERS analysis of the characteristic spectrum of 4-MBA, a Raman reporter, on the SERS tags is monitored with a modular Raman spectrometer with a fibre-optic Raman probe.

Experimental

Chemicals and Instruments

Cetyltrimetylammonuim bromide (CTAB), gold (III) chloride trihydrate ($HAuCl_4 \cdot 3H_2O$, 99 %), sodium borohydride ($NaBH_4$, 98 %), silver nitrate ($AgNO_3$, 99 %), ascorbic acid, glycine, sodium hydroxide (NaOH), magnesium chloride ($MgCl_2$), D-(+)-glucose (99.5 %), 1-ethyl-3-(3-dimethylaminopropyl) carbodiimide (EDC), 3-sulfo-N- hydroxysuccinimide (sulfo-NHS), bovine serum albumin (BSA) and 4-mercaptobenzoic acid (4-MBA) were obtained from Sigma-Aldrich (MO, USA, http://www.sigma aldrich.com). Dulbecco's Phosphate Buffered Saline (DPBS) and foetal bovine serum (FBS) were purchased from Invitrogen (NY, USA, http://www.invitrogen.com). mPEG-SH (MW5000) was purchased from Laysan Bio Inc. (AL, USA). FluidMAG-CMX, 200 nm-magnetic nanoparticles, were purchased from Chemicell (Berlin, Germany). SERS measurements were performed using a HORIBA modular Raman spectrometer with a 785 nm Raman fibre optic probe (CA, USA). Ultra-high vacuum (UHV) aluminium foil was purchased from All Foils, Inc. (PH, USA). The oligonucleotides with high-pressure liquid chromatography (HPLC) purification were purchased from Integrated DNA Technologies (Singapore, http://sg.idtdna.com) and used

without further modification. The sequence of the DNA probes and target miRNAs are shown in table 1.

Table 1 List of oligonucleotides

Name	Sequence
capture DNA probe	5' - AGA TGG TGC TAT TTT TTT TTT– amine - 3'
reporter DNA probe	5' - Thiol-TTT TTT TTT TTA ACC GAT TTC- 3'
miR-29a	5' - uag cac cau cug aaa ucg guu a - 3'
miR-21	5' - uag cuu auc aga cug aug uug a - 3'
miR-210	5' - cug ugc gug uga cag cgg cug a - 3'

Preparation of SERS tags

Gold nanorods (AuNRs) were synthesised according to a slightly modified seed-mediated growth method described Previously.[43] After synthesis, AuNRs were characterised by UV-VIS absorption (Power wave XS2, Bio-Tek, USA) and transmission electron microscope (TEM, JEM 2100, JEOL, Japan). Then, SERS tags were prepared by attaching Raman molecules, 4-mercaptobenzoic acid (4-MBA), reporter DNA probes, and polyethyleneglycol (mPEG-SH) on the surface of AuNRs through a self-assembly process similar to the previous report.[44] Briefly, 500 µL of the stock AuNRs solution was centrifuged at 10,000 RPM for 5 minutes to remove the stabilising CTAB bilayers. Next, the pellet was redispersed in 1 mL of 0.5 mM CTAB and subsequently mixed with 5.0 µL of 20 mM 4-MBA in DMSO for 6 h on a rotator mixer at room temperature. The unbound 4-MBA was removed by centrifugation at 10,000 RPM for 10 min. The 4-MBA coated AuNRs pellet was resuspended in 2 mM CTAB (500 µL). DNAse free water (500 µL) was added to the above solution. Freshly prepared mPEG-SH solution (2 mM mPEG-SH-5000, 100 µL in DNAse free water) was also added to stabilise and functionalised the coated AuNRs. Subsequently, 10 µM reporter DNA probes (32 µL) were added and incubated for 12 h at room temperature in the dark. The resultant SERS tags were recovered by centrifugation at 10,000 rpm for 10 min and redispersed in DNAse free water.

Preparation of capture probe

Carboxylated magnetic nanoparticles (MNPs) were activated prior to conjugation using carbodiimide chemistry to prepare the surface for covalent conjugation with amine-modified capture DNA probes. Briefly, 4.0 µL of MNPs (25 mg/mL) was mixed with 0.1 mg EDC and 0.1 mg sulfo-NHS in 500 µL of 15 mM MES buffer (pH 5.5). The
mixture was left to react for 15 min on a rotator mixer at room temperature. The excess EDC and NHS were removed by magnetic separation. Then, 500 µL of 10 mM PBS (pH 7.4) was added and mixed thoroughly to disperse the activated MNP, followed by adding 10 µM reporter DNA probes (5.0 µL). The mixture was incubated for 12 h on a rotator mixer at 4 °C. The magnetic conjugates were washed 3 times, then resuspended in 10 mM PBS 100 µL and stored at 4°C until used.

Detection of target miRNA

In a typical experiment, target miR-29a at different concentrations (10 µL) was mixed with capture DNA conjugated MNPs (5.0 µL) in 85 µL of hybridisation buffer containing 10 mM PBS and 0.1% BSA. The mixture was incubated for 30 min on a rotator mixer at

Fig. 1 Schematic of magnetic capture-SERS platform for miRNA detection

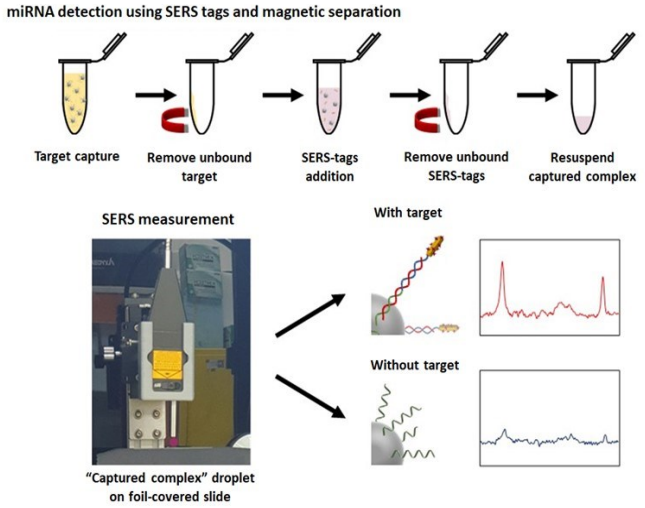

room temperature, followed by the addition of washing buffer (0.1% Tween 20 in 10 mM PBS) and sonication. The unbound target

miRNAs were removed through magnetic separation. The MNP-miRNA complexes were resuspended in 80.0 µL of hybridisation buffer. Then, SERS tags containing reporter DNA probes (20.0 µL) were added to the mixture and incubated for another 30 min on a rotator mixer at room temperature. The hybridised MNP-miRNA-SERS tag complex was concentrated with a magnet and washed 3 times. Finally, the complexes were resuspended in 20.0 µL of DNAse free water for SERS analysis.

SERS analysis

The concentrated MNP-miRNA-SERS tag complex (5 µL) was dropped onto a glass microscope slide covered with UHV aluminium foil to form a microdroplet. SERS measurements were performed on the liquid microdroplet using a HORIBA modular Raman spectrometer with 785 nm excitation and Raman fibre optic probe. A piece of silicon substrate on a glass microscope slide was used to calibrate and to fix the laser focus distance for subsequent measurements. The laser power was set at 0.75 mW and applied to the centre of the sample microdroplet. The exposure time was 60 s with 3 accumulations, and the detection range was 800-1800 cm^{-1}. SERS spectra were collected from 3 samples for each concentration and 3 times for each sample.

Results and discussion

The principle of the SERS-based miRNA detection platform is based on specific target-induced sandwich complex formation, as schematically illustrated in Fig. 1. SERS tags and magnetic nanoparticles were functionalised with complementary DNA probes specific to target the miRNA of interest. Upon addition of MNPs conjugated with complementary DNA probes, the target miRNA is captured and then labelled with SERS tags conjugated with complementary reporter DNA through a specific hybridisation. The resultant hybridisation complexes are magnetically concentrated and separated for the SERS measurement. The SERS tags assembly creates multiple 'hotspots' that enhance electromagnetic radiation of Raman molecules coated on the AuNRs. Thus, an intense SERS signal occurred in the presence of the target. When there is no target, the hybridisation complex cannot be formed, and the SERS tags will be washed away after magnetic separation, resulting in the absence of the SERS signal.

Fabrication and Characterisation of SERS tags and capture probes

The selection of metallic nanomaterial for SERS tag fabrication is an important factor that can affect strong SERS signal and reflect the high sensitivity of SERS-based detection. Anisotropic nanoparticles such as stars, cubes, triangles, and rods were reported to provide a concentrated electromagnetic field at the tips, which generate an intense SERS signal. This study selected AuNRs as a metallic substrate for SERS tag fabrication due to its strong light absorption and scattering properties. The AuNRs were synthesised by a modified seed-mediated growth method using CTAB as a building block, in which their aspect ratio can be tuned by adjusting the ratio of surfactants and silver nitrate.[43,44] The characteristic absorption spectrum and TEM image of the synthesised AuNRs are shown in Fig. 2a. The AuNRs have an aspect ratio of 2.76 with an average width of 17±2 nm and length of 47±2 nm, respectively. As seen in Fig. 2a, the AuNRs showed a weak plasmon band at 516 nm from the transverse electron oscillation and a strong longitudinal band from the longitudinal electron oscillation at 708 nm.

The SERS tags were then fabricated from the AuNRs using a self-assembly process as depicted in Fig. 2b. Briefly, the as-prepared AuNRs were centrifuged to remove CTAB bilayers on their surface. Subsequently, a Raman reporter containing a thiol group, 4-mercaptobenzoic acid (4-MBA), was attached to the available AuNRs surface through a thiol-gold interaction defined as AuNRs-4-MBA. Then, the reporter DNA sequence complementary to part of the target miR-29a was conjugated to AuNRs-4-MBA and ascribed as SERS tags. The reporter DNAs consist of the target recognition part, poly-T (thymine) as a spacer, and a thioalkane hydrocarbon at the 5' end. The target recognition part contains 11 bases that can specifically hybridise with half of the target miR-29a (Table 1). The poly-T spacer extends the recognition unit from the surface of AuNRs to avoid steric hindrance of the SERS tags while interacting with the target miRNA. The hydrocarbon containing a thiol unit at the 5'end allows self-assembly of reporter DNA

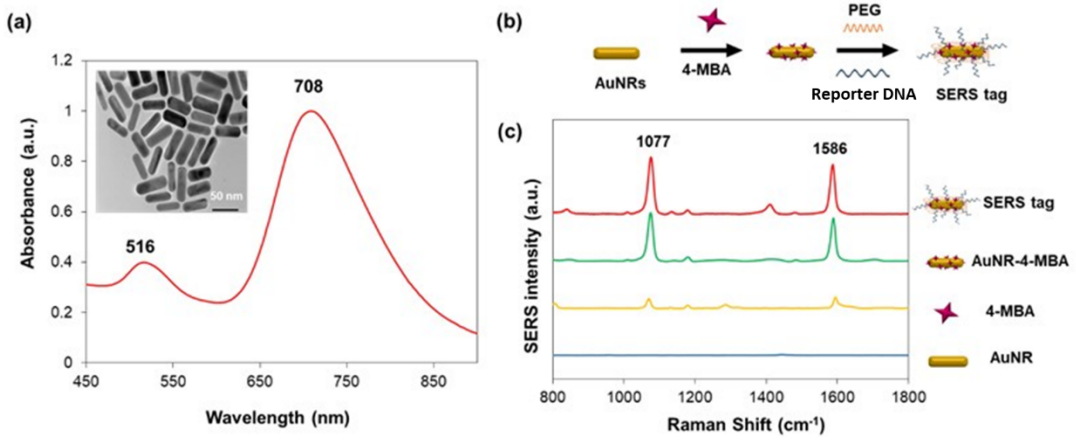

Fig. 2 Char ɜs fabrication using self-a Rs, 10 mM 4-MBA, AuN

onto AuNRs-4-MBA. In addition, polyethylene glycol (PEG) was added during the DNA conjugation process to passivate the particle surface to minimise aggregation and nonspecific interaction.

The spectra of SERS tags for each fabrication step were then evaluated using a light source at the wavelength of 785 nm. As demonstrated in Fig. 2c, the bare AuNRs do not show any Raman shift as a background. In contrast, 10 mM of 4-MBA solution showed characteristic peaks at 1077 and 1586 cm^{-1} assigned to the C-S stretching mode and aromatic ring breathing mode of C-C, respectively. After 4-MBA was encoded on the AuNRs surface, AuNRs-4-MBA exhibited a strong SERS signal. The intensification was ascribed to the localised electromagnetic field of electrons on the AuNRs surface combined with the charge transfer effect between metal and 4-MBA molecules. After subsequent attachment of DNA reporter probes, a similar pattern of SERS spectra was observed on the SERS tags with comparably high intensity. Moreover, successful SERS tag fabrication was also determined by comparing the zeta potential of the particle surface for each step of modification.

The as-prepared AuNRs possessed the zeta potential of 23.2±0.6 mV due to the presence of the highly positive charge surfactant, CTAB, to stabilise the AuNRs surface. After 4-MBA was encoded, the surface charge AuNRs-4-MBA became negative (-21.9±0.6 mV) due to the high density of carboxyl groups from 4-MBA. Upon DNA probe conjugation, the zeta potential of SERS tags changed to -12.6±2.0 mV. The strong ion pairing of the phosphate groups from DNA with cations shields the negative charge, hence the increase in the zeta potential was observed. The changes of surface charge in each step of modification indicated the successful SERS tag fabrication groups from 4-MBA. The changes of surface charge in each step of modification indicated the successful SERS tag fabrication using a self-assembly process. The capture DNA probes were prepared by functionalising magnetic nanoparticles with the complementary DNA sequence to recognise the target miR-29a. The capture DNA comprises of 11 bases that can hybridise with half of the target miR-29a as demonstrated in Table 1. The poly-T spacer was added to the capture probe sequence to avoid steric hindrance of the conjugates similar to the reporter DNA probe. The amine group at the 3'end facilitates the coupling of the capture DNA probes with the carboxylated magnetic nanoparticles through carbodiimide chemistry. The successful capture probes preparation was also confirmed through the reduction of the total negative charge of carboxylated magnetic nanoparticles from -15.43±0.75 mV to -11.70±0.61 mV after DNA conjugation. The magnetic conjugates were then used to capture the target miR-29a, followed by SERS tags labelling described in the scheme previously. The sandwich complexes can be magnetically concentrated by an external magnet. The unbound SERS tags can be removed at this step. This separation process can increase the purity of the target by reducing interference and concentrating a limited target in the samples for efficient interrogation.

SERS-based miRNA detection

To demonstrate proof-of-the-concept, SERS detection of the target miRNA was conducted by incubating a sample containing 1 µM of miR-29a with the MNPs conjugated DNA capture probes for 30 min. After washing steps, SERS tags were added to the MNP-miRNA for sandwich complex formation and labelling, followed by another 30 min incubation. The washing steps were performed by adding wash buffers, brief sonication, and magnetic separation to remove unbound SERS tags. Upon SERS measurement, an intense characteristic spectrum of 4-MBA was recorded, as demonstrated in Fig. 3.

Simultaneously, a low background signal of 4-MBA was observed in the negative control that contained no miR-29a. The strong SERS intensity indicated the presence of the target miR-29a, which induced MNP-miRNA-SERS tag sandwich complex formation through specific hybridisation of the target miRNA and complementary probes on the MNPs and SERS tags. While the negative control without the target miRNA showed minimum nonspecific interaction indicated by the low SERS signal as a background after washing steps by magnetic separation. All the SERS-tags were washed away, and only the capture probes remained in the system. The SEM images and EDX analysis of the MNP-miRNA-SERS tag sandwich complex formation in the presence of miR-29a were also shown in the supplementary material (Fig.S1). Based on this result, the system provides a strong detection signal and a high degree of specificity suitable for further investigation.

The performance of the system was evaluated using various concentrations of miR-29a (0 – 1000 pM). At the concentration of 1000 pM target miR-29a, a strong SERS signal corresponding to the characteristic spectra of 4-MBA is observed. The intensity of the SERS signal decreased proportionally when the concentration of the target miR-29a was reduced, as shown in Fig. 4a. This result indicated that the degree of MNP/miR-29a/SERS tag sandwich complex formation is directly related to the target miRNA

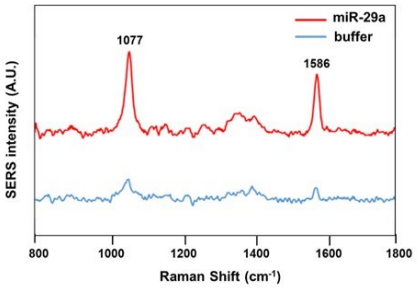

Fig. 3 SERS s
and buffer a
M miR-29a

concentration reflected by corresponding changes in SERS intensity. The linear relationship between the concentration of miR-29a

and SERS intensity in the range of 0-1000 pM was observed (Fig. 4b). The linear equations are y = 72.2X – 11.5 with an R^2 of 0.9289, and y = 68.1X – 40.5 with an R^2 of 0.93889 for the Raman shift at 1077, and 1586 cm^{-1}, respectively. Additionally, the lowest detectable concentration of miR-29a using this system was ca. 10 pM without any other amplification steps.

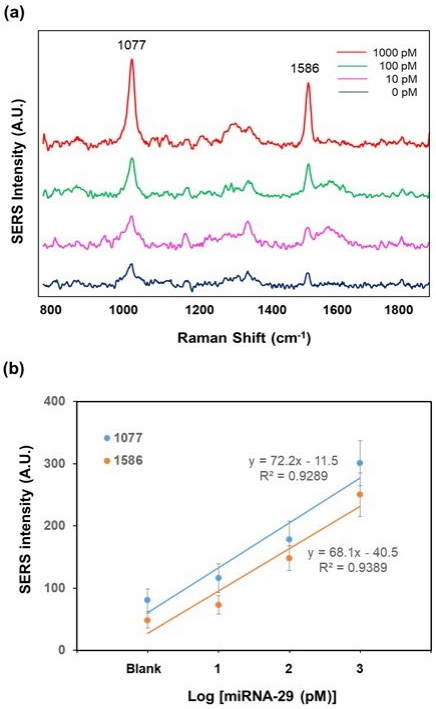

Fig. 4 Sensitivity of miR-29a detection (a) SERS spectra of miR-29a with various concentrations (b) Plot of SERS intensity at 1077 and 1586 cm^{-1} versus concentration of miR-29a.

To evaluate the selectivity of this SERS-based miRNA detection, two different sequences from miR-29a were used as non-targets. The measurements were conducted under similar conditions and concentrations of 100 pM. Simultaneously, only SERS tags incubated with MNP capture probes in the absence of target miRNA were assigned as a blank. After SERS measurement, the intensity of the dominant 1077 ($I_{1077,s}$) and 1586 ($I_{1586,s}$) cm^{-1} peaks of the samples containing the target, miR-29a, and non-targets, miR-21 and miR-210, were subtracted from the peak intensities of the blank (in the absence of the target, $I_{1077,b}$ and $I_{1586,b}$) and normalised with the intensity of the SERS-tag. Both of the non-targets showed a much lower level of peak intensity compared to the target after blank subtraction, as demonstrated in Fig. 5. This result suggests a high-level target detection selectivity by the assay.

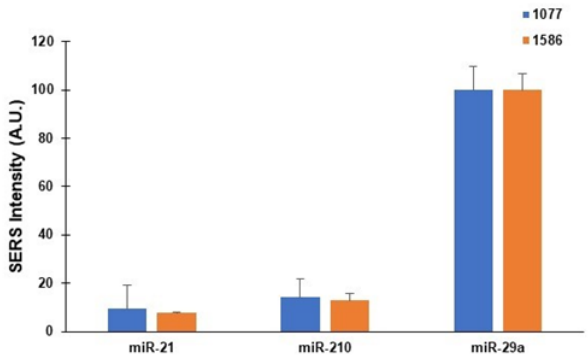

Fig. 5 Selectivity of the SERS based-platform for the detection of 100 pM miR-29a compared to 100 pM non-target miRNAs.

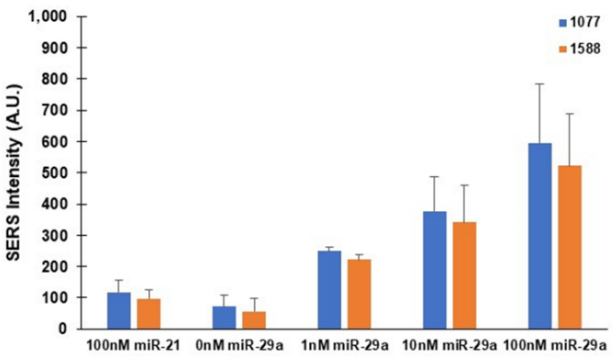

T

Fig. 6 Feasibility for the detection of miR-29a in complex media containing 10% FBS in 10 mM PBS compared to the non-target miR-21.

The ability of this SERS-based miRNA detection assay in complex media was further evaluated. Here, a hybridisation buffer containing 10% fetal bovine serum (FBS) in 10 mM PBS was used to simulate the complex biological environment. Different concentrations of miR-29a (0-100 nM) were used to determine the assay sensitivity, and the non-target miR-21 (100nM) was used to determine the assay selectivity in complex media. The SERS intensity of the dominant 1077 and 1586 cm^{-1} peaks of the samples containing different concentrations of the target miR-29a and non-target miR-21 were demonstrated in Fig. 6. Here, the peak intensities for the target miR-29a increased as the concentration of miR-29a increased. Meanwhile, the peak intensities of the non-target miR-21 remained relatively low and comparable to the peak intensities when there was no target miRNA. This result demonstrated that this SERS-based miRNA detection assay is feasible for miRNA analysis in complex media.

Conclusions

We have successfully demonstrated a new platform for miRNA detection using a SERS-based assay combined with a magnetic separation step. A biomarker for multiple cancers, miR-29a, was selected as a model target. The target was first captured by MNPs conjugated with the capture DNA probe to recognise the miR-29a sequence, followed by the SERS tags labelling through hybridisation to the target. The sandwich complexes of MNP/miR-29a/SERS tags were formed and magnetically separated for SERS analysis. SERS tags assembled through the sandwich complex formation creates multiple 'hotspots' that intensify the SERS signal due to the presence of the target. Consequently, a SERS response proportional to the concentration of the target miR-29a with high selectivity was observed. The recorded LOD of the system is estimated to be 10 pM, which is comparable to other similar works that use only one type of plasmonic nanoparticles without amplification step.[39,45-46] Although previous reports have shown SERS-based assays with superior sensitivity, those methods often require enzymatic reaction, amplification steps, more than one plasmonic materials, complicated SERS tags preparation, including need a confocal Raman spectrometer which hinder the use at point-of-care or at a low resource facility.[29, 37-38, 45-50] Our SERS tags can be simply fabricated using a self-assembly process. The assay can be performed within only two steps. Furthermore, our SERS based assay can detect target miRNAs in complex media, thus demonstrating its potential to be used as a detection platform for medical diagnostics. Lastly, our SERS based assay can be analysed with a modular Raman spectrometer and a fibre optic Raman probe by dropping a microvolume sample on a microscope slide covered with UHV aluminium foil. This small volume required for sample analysis makes this method suitable for detection of very low abundance target molecules such as miRNA.

Author Contributions

Kiatnida Treerattrakoon: Investigation, methodology, result analysis, and writing–original draft and editing. Pimporn Roeksrungruang: methodology. Tararaj Dharakul: supervision. Deanpen Japrung: supervision. Karen Faulds: supervision. Duncan Graham: supervision, writing review and editing. Suwussa Bamrungsap: conceptualization, supervision, methodology, validation, resources, writing, review and editing, project administration, and funding acquisition.

Conflicts of interest

There are no conflicts to declare.

Acknowledgements

This work was supported by a grant from Thailand Research Fund (TRF) [grant number TRG6080003] and the National Nanotechnology Center (NANOTEC), Thailand.

References

1 V. de Guire, R. Robitaille, N. Tétreault, R. Guérin, C. Ménard, N. Bambace and P. Sapieha, *Clin. Biochem.*, 2013, **46**, 846–60.
2 M. I. Almeida, R. M. Reis and G. A. Calin, Mutation Research - Fundamental and Molecular Mechanisms of Mutagenesis, 2011, **717**, 1–8.
3 J. Feng, W. Xing and L. Xie, *Int. J. Mol. Sci.*, 2016, **17**, 1–12.
4 R. Jiménez-Lucena, A. Camargo, J. F. Alcalá-Diaz, C. Romero-Baldonado, R. M. Luque, B. van Ommen, J. Delgado-Lista, J. M. Ordovás, P. Pérez-Martínez, O. A. Rangel-Zúñiga and J. López-Miranda, *Exp Mol Med,* 2018, **50,** 1-12.
5 J. Pordzik, D. Jakubik, J. Jarosz-Popek, Z. Wicik, C. Eyileten, S. de Rosa, C. Indolfi, J. M. Siller-Matula, P. Czajka and M. Postula, *Cardiovasc Diabetol.*, 2019, **18**, 1–19.
6 S. P. R. Romaine, M. Tomaszewski, G. Condorelli and N. J. Samani, *Heart*, 2015, **101**, 921–928.
7 S. S. Zhou, J. P. Jin, J. Q. Wang, Z. G. Zhang, J. H. Freedman, Y. Zheng and L. Cai, *Acta Pharmacol Sin.*, 2018, **39**, 1073–1084.
8 Y. Gómez-gómez, J. Organista-nava and P. Gariglio, *Biomed Res. Int*, 2013, 1–15.
9 Y. Han, G.-X. Xu, H. Lu, D.-H. Yu, Y. Ren, L. Wang, X.-H. Huang, W.-J. Hou, Z.-H. Wei, Y.-P. Chen, Y.-G. Cao and R. Zhang, *Int. J. Clin. Exp. Pathol.*, 2015, **8**, 7131–7139.
10 W. Jia, Y. Wu, Q. Zhang, G. Gao, C. Zhang and Y. Xiang, *Mol Clin Oncol.*, 2015, 851–858.
11 D. Zheng, S. Haddadin, Y. Wang, L. Q. Gu, M. C. Perry, C. E. Freter and M. X. Wang, *Int. J. Clin. Exp. Pathol.*, 2011, **4**, 575–586.
12 M.-H. Mo, L. Chen, Y. Fu, W. Wang and S. W. Fu, *J Cancer.*, 2012, **3**, 432–448.
13 J. Gyoba, S. Shan, W. Roa and E. L. R. Bédard, *Int. J. Mol. Sci.*, 2016, **17**, 1–14.
14 S. Srivastava, A. Bhardwaj, S. Leavesley, W. Grizzle, S. Singh and A. Singh, *Biotec Histochem.*, 2013, **88**, 373–387.
15 A. Válóczi, C. Hornyik, N. Varga, J. Burgyán, S. Kauppinen and Z. Havelda, *Nucleic Acids Res.*, 2004, **32**, 1-7.
16 D. D. Duncan, M. Eshoo, C. Esau, S. M. Freier and B. A. Lollo, *Anal. Biochem.*, 2006, **359**, 268–270.
17 R. C. Thompson, M. Deo and D. L. Turner, *Methods*, 2007, **43**, 153–161.
18 J. J. Zhao, J. Yang, J. Lin, N. Yao, Y. Zhu, J. Zheng, J. Xu, J. Q. Cheng, J. Y. Lin and X. Ma, *Childs Nerv Syst.*, 2009, **25**, 13–20.
19 A. J. Qavi, J. T. Kindt and R. C. Bailey, *Anal Bioanal Chem.*, 2010, **398**, 2535–2549.
20 J. Ye, M. Xu, X. Tian, S. Cai and S. Zeng, *J. Pharm. Anal.*, 2019, **9**, 217–226.
21 C. Li, Z. Li, H. Jia and J. Yan, *Chem. Commun.*, 2011, **47**, 2595–2597.
22 S. P. Jonstrup, J. Koch and J. Kjems, *RNA*, 2006, **12**, 1747–1752.
23 K. Treerattrakoon, T. Jiemsakul, C. Tansarawiput, P. Pinpradup, T. Iempridee, P. Luksirikul, K. Khoothiam, T. Dharakul and D. Japrung, *Anal. Biochem.*, 2019, **577**, 87–97.
24 K. Khoothiam, K. Treerattrakoon, T. Iampridee, P. Luksirikul, T. Dharakul and D. Japrung, *Analyst*, 2019, **144**, 4180–4187.
25 X. Miao, X. Ning, Z. Li and Z. Cheng, *Sci Rep*, 2016, **6**, 32358.
26 M. Schechinger, H. Marks, A. Locke, M. Choudhury and G. Coté, *Journal of Biomedical Optics*, 2018, **23**, 017002.
27 R. Li, B. Gui, H. Mao, Y. Yang, D. Chen and J. Xiong, *ACS Sens.*, 2021, **18**, 23.
28 S. Lu, T. You, N. Yang, Y. Gao and P. Yin, *Analytical and Bioanalytical Chemistry*, 2019, **412**, 1159–1167.
29 X. Song, T. Xu, Y. Song, X. He, D. Wang, C. Liu and X. Zhang, *Talanta*, 2020, **218**, 121206.
30 S. Mabbott, S. C. Fernandes, M. Schechinger, G. L. Cote, K. Faulds, C. R. Mace and D. Graham, *Analyst*, 2020, **145**, 983–991.
31 A. Paudel, D. Raijada and J. Rantanen, *Adv. Drug Deliv. Rev.*, 2015, **89**, 3–20.
32 O. Stevens, I. E. I. Petterson, J. C. C. Day and N. Stone, *Chem. Soc. Rev*, 2016, **45**, 1919.
33 J. D. Driskell, O. M. Primera-Pedrozo, R. a Dluhy, Y. Zhao and R. a Tripp, *Appl. Spectrosc.*, 2009, **63**, 1107–14.
34 D. Graham, D. G. Thompson, W. E. Smith and K. Faulds, *Nat. Nanotechnol.*, 2008, **3**, 18–21.
35 X. Qian, X. Zhou and S. Nie, *J. Am. Chem. Soc.*, 2008, **130**, 14934–14935.
36 B. Guven, F. C. Dudak, I. H. Boyaci, U. Tamer and M. Ozsoz, *Analyst*, 2014, **139**, 1141–7.
37 H. Zhang, Y. Yi, C. Zhou, G. Ying, X. Zhou, C. Fu, Y. Zhu and Y. Shen, *RSC Adv.*, 2017, **7**, 52782–52793.
38 H. Zhang, C. Fu, S. Wu, Y. Shen, C. Zhou, J. Neng, Y. Yi, Y. Jin and Y. Zhu, *Anal. Methods.*, 2019, **11**, 783–793.
39 A. Yamada, T. Horimatsu, Y. Okugawa, N. Nishida, H. Honjo, H. Ida, T. Kou, T. Kusaka, Y. Sasaki, M. Yagi, T. Higurashi, N. Yukawa, Y. Amanuma, O. Kikuchi, M. Muto, Y. Ueno, A. Nakajima, T. Chiba, C. R. Boland and A. Goel, *Clinical Cancer Research*, 2015, **21**, 4234–4242.
40 Y. Pei, Y. Lei and X. Liu, *Biochimica et Biophysica Acta - Molecular Basis of Disease*, 2016, **1862**, 2177–2185.
41 R. Bargaje, S. Gupta, A. Sarkeshik, R. Park, T. Xu, M. Sarkar, M. Halimani, S. S. Roy, J. Yates and B. Pillai, *PloS one*, 2012, **7**, e43243.
42 Y. Li, Z. Wang, Y. Li and R. Jing, *Oncol Lett.*, 2017, **13**, 3896–3904.
43 B. Nikoobakht and M. A. El-Sayed, *Chem. Mater.*, 2003, **15**, 1957–1962.
44 S. Bamrungsap, A. Treetong, C. Apiwat, T. Wuttikhun and T. Dharakul, *Microchim Acta*, 2016, **183**, 249–256.
45 Y. Song, T. Xu, L.-P. Xu, X. Zhang, R. Li, / Chemcomm and C. Communication, *Chem. Commun*, 2019, **55**, 1742.
46 H. Zhang, Y. Liu, J. Gao and J. Zhen, *Chem. Commun*, 2015, **51**, 16836.
47 H. T. Ngo, H. N. Wang, A. M. Fales, B. P. Nicholson, C. W. Woods and T. Vo-Dinh, *Analyst*, 2014, **139**, 5655–5659.
48 M. Schechinger, H. Marks, S. Mabbott, M. Choudhury and G. Cote', *Cite this: Analyst*, 2019, **144**, 4033.
49 J. Su, D. Wang, L. Nörbel, J. Shen, Z. Zhao, Y. Dou, T. Peng, J. Shi, S. Mathur, C. Fan and S. Song, *Analytical Chemistry*, 2017, **89**, 2531–2538.
50 L. Ye, J. Hu, L. Liang and C.-Y. Zhang, *Chem. Commun*, 2014, **50**, 11883.